Analytical results for the wrinkling of graphene on nanoparticles

M. Guedda,[1,*] N. Alaa,[2] and M. Benlahsen[3]

[1]*LAMFA, CNRS-UMR 7352, Université de Picardie Jules Verne, Amiens, France*
[2]*LAMAI, FST Gueliz Cady Ayyad University, Marrakech, Morocco*
[3]*LPMC, Université de Picardie Jules Verne, Amiens, France*

A continuum elastic model, describing the wrinkling instability of graphene on substrate-supported silica nanoparticles [M. Yamamoto *et al.*, Phys. Rev. X **2**, 041018 (2012)], is analytically studied, and an exact analytical expression of the critical nanoparticle separation or the maximum wrinkle length is derived. Our findings agree with the scaling property of Yamamoto *et al.* but improve their results. Moreover, from the elastic model we find a pseudomagnetic field as a function of the wrinkling deflection, leading to the conclusion that the middle of the wrinkled graphene may have a zero pseudomagnetic field, in marked contrast with previous results.

I. INTRODUCTION

Graphene, which is considered one of the most promising materials in the 21st century, is a two-dimensional membrane with remarkable thermal and electronic and unusual structural and mechanical properties. These make it especially interesting for many theoretical and experimental studies for different applications ranging from nanoelectronics to biological tissues.

A freestanding graphene is nonflat and has a tendency to be crumpled, so graphene is often used with a substrate. Once transferred on a flat surface, or further suspended, the membrane exhibits complex responses to external forces or geometrical constraints, such as wrinkling and delimitation behaviors, that may lead to unpredictable graphene properties and/or mimic the effect of a magnetic field on graphene's electronic structure [1–5]. Therefore, it is important to know whether or not the graphene sheet can conform to the subtract, and to build a theoretical model to predict how a graphene sheet deforms in response to stretching and bending forces for a successful technological graphene implementation or wrinkle and delamination manipulations.

Graphene, which is also used in lithium ion battery anodes, has also opened new possibilities for the storage of more lithium ions and (then) for the increase of the battery's capacity. As potential high-performance anode materials [6], nanocomposites of silicon nanoparticles are dispersed between graphene layers to keep them dispersed without aggregation. It is found that when a small Si nanoparticle intercalates between a graphene bilayer, each layer wraps around the Si nanoparticle, forming a conical dome in graphene, and when two neighboring Si nanopraticles intercalate between two graphene layers, the wrinkling pattern in graphene can evolve dynamically. Zhu *et al.* [6] have determined a critical dispersion distance between Si nanoparticles below which Si nanoparticles between two graphene layers evolve to bundle together. In particular, it is shown that there is an approximately linear dependence of critical dispersion distance on the nanoparticle size.

Yamamoto *et al.* [4] studied the effect of the spacial structure of the substrate on the morphology of the graphene. More precisely, they reported on experimental studies of the wrinkling of a graphene membrane supported on SiO_2 substrates with randomly placed topographic perturbations produced by SiO_2 nanoparticles with density ρ_{np}. This study showed that ρ_{np} has a direct influence on the wrinkling pattern in graphene. In the limit of small effective mechanical thickness graphene, it is observed that when ρ_{np} is low, the monolayer graphene detaches from the substrate only in a small region around the nanoparticles. As ρ_{np} increases, wrinkles or ridges form connecting pairs of protrusions. An analytical approach has also been developed to discuss the critical ridge length, χ_c (i.e., the maximal distance between two nanoparticles), at which a transition between a wrinkling and a partial or complete delamination occurs. It was found that χ_c varies linearly with the nanoparticle size. Zhu and Li [7] proposed molecular dynamics simulations to investigate the graphene morphology regulated by nanoparticles on a substrate. It is found that the wrinkling formation in graphene depends not only on the distance between two neighboring nanoparticles but also on the nanoparticle size in agreement with the experimental observation of Ref. [4].

Despite experimental and theoretical investigations, some aspects of the results of Ref. [4] remain to be elucidated. For example, it was found that the profile of wrinkling is described in terms of an explicit singular function (see below). However, it is not clear why this singular solution is energetically favorable and/or why the associated ridge length is the maximum distance between two nanoparticles. Our initial aim here is not to consider a different physical model or to introduce another intuitive or speculative scenario. Rather, the continuum elastic model describing the wrinkling and the critical nanoparticle separation are analytically worked out in detail. Our results agree with the scaling behaviors of Yamamoto *et al.*, but show that the ridge running along the wrinkle between two nanoparticles follows a smooth catenary-like profile and improves the critical wrinkle length.

II. THE PHYSICAL CONTEXT

A brief presentation of the previous results may be appropriate. The thin plate and membrane theories have a long

*guedda@u-picardie.fr
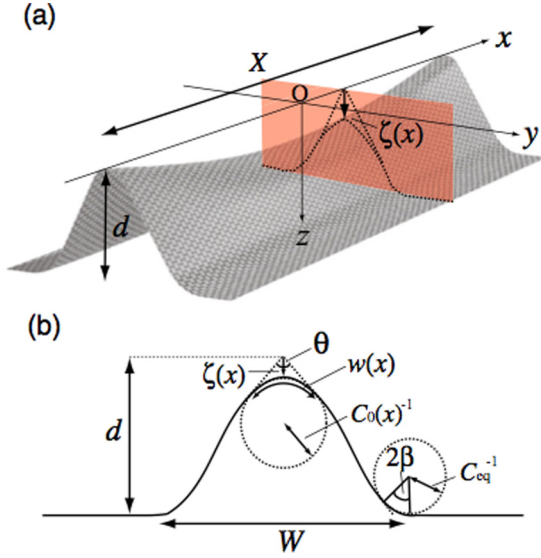
FIG. 1. Schematic of a wrinkle according to Ref. [4]. (a) Deformation of graphene membrane between two nanoparticles with diameters d. (b) The wrinkle profile along the transverse direction. The diameter d, dihedral angle θ, ridge length χ, and the base of the wrinkle profile, $W = d \tan(\theta/2)$, are indicated. The curvature radius $\mathcal{C}_0^{-1}$ and the width of the deformed region w are connected to deflection ζ via $\mathcal{C}_0^{-1} = [\frac{1}{\sin(\theta/2)} - 1]^{-1}\zeta, w = (\pi - \theta)[\frac{1}{\sin(\theta/2)} - 1]^{-1}\zeta$.

history, and deformations of elastic sheet thins are classical subjects of continuum mechanics. The problem has been studied from different points of view, and different types of deformations or surface instabilities and a possible continuous or discontinuous transition between them have been predicted (critical conditions). Most deformations (buckle delamination, wrinkling, cracking, or fracture, etc.) are viewed as (local) minimizers of suitable elastic energies. However, due to the complexity of the equations (fourth-order partial differential equations, boundary layer, free boundary conditions, etc.) that describe surface morphologies, rigorous proofs are in most cases difficult to achieve, and since explicit solutions exist only in a few cases, numerical treatments are inevitable.

In Ref. [4] the elastic analytical approach supposes that the ridge, running along the wrinkle between two nanoparticles with diameter d separated by χ, follows a catenary-like profile, à la Robert Hooke (1675), with a deflection $\zeta = \zeta(x)$ (from the original ridge line) and a maximum deflection $\zeta_0 = \zeta(0)$, as depicted in Fig. 1. The profile of the ridge along the transverse direction is described by the curvature radius $\mathcal{C}_0^{-1} = \mathcal{C}_0^{-1}(x)$ and the opened angle θ, which is assumed to be independent of x.

The catenary-like profile, which was used by Lobkosvky *et al.* [8] to find the scaling energy properties of a crumpled elastic sheet, allowed an easy analytical treatment. More precisely, from the equilibrium equation, it is argued that the graphene profile can be described in terms of the deflection

$$\zeta^{\text{ex}} = \left(\frac{27\kappa}{4E_{2D}}\right)^{1/6}\left[\frac{1}{\sin(\theta/2)} - 1\right]^{1/3}\left(\frac{\chi}{2} - |x|\right)^{2/3}, \quad (1)$$

where $E_{2D} = Yh/(1 - \nu^2)$ is the tensile rigidity, $\kappa = Yh^3/12(1 - \nu^2)$ is the bending rigidity, Y is the Young's modulus, h is the thickness, and ν is Poisson's ratio of graphene. The ridge length is given by

$$\chi = \zeta_0^{3/2}\left(\frac{64E_{2D}}{27\kappa}\right)^{1/4}\left[\frac{1}{\sin(\theta/2)} - 1\right]^{-1/2} \equiv \chi^{\text{ex}}. \quad (2)$$

The above explicit solution is the key element of the analytical results presented in Ref. [4]. This solution is used to derive the critical ridge length χ_c as a function of the nanoparticle size d. It was also used to evaluate the strain distribution [$\varepsilon_x \sim (\kappa/E_{2D})^{1/3}(\chi/2 \mp x)^{-2/3}$] and strain pseudomagnetic fields in a wrinkle. In particular, it is found that the pseudomagnetic field has, in the middle of a wrinkle, a broad minimum on the order of 10 T for $\chi = 100$ nm.

While this approach is interesting and allows one to have far-reaching physical intuition, the explicit solution presents a discontinuity of the slope at $x = 0$, and then it does not necessarily follow a caternay-like profile. Hence, relationship (2), which is directly derived from (1), could be incorrect.

From a mathematical point of view, a natural question is whether there exists a smooth minimizer solution for the one-dimensional elastic energy (see below). Responses of this innocent and naive remark may affect significantly the prediction of the critical ridge length and other graphene properties such as strain and pseudomagnetic fields.

Regarding the aforementioned points, the present purpose, as mentioned in the Introduction, is to present a mathematical study of the wrinkling of graphene on nanoparticles by reexamining the equilibrium equation, with a view to identifying a smooth (local) minimizer deflection of the elastic energy. Our approach is based on the work of Ref. [4], though we differ in our treatment of the equilibrium equation. We are able to present a complete picture of solutions, including singular solution (1), by varying the maximum deflection and the slope at $x = 0$. We then identify the unique smooth critical deflection (we require only the continuity of the slope) leading to critical distance χ_c and discuss some physical properties. We shall see that the minimizer deflection can be expressed in terms of the inverse of an incomplete normalized beta function and that χ_c can be derived in an explicit form. Interesting, our analysis shows that it is unnecessary to find explicitly the critical deflection to determine χ_c. In addition, we easily observed, from the continuum elastic model, that the pseudomagnetic field can be calculated as a function of the critical deflection, and then a zero pseudomagnetic field can be located in the middle of the wrinkled graphene, in a marked contrast to Ref. [4].

III. PRELIMINARY RESULTS

To facilitate our study and to put the mathematical discussion into the graphene instability context, we give here a brief description of the approach of Yamamoto *et al.* The geometry of Fig. 1 presents a schematic of a wrinkled graphene. This relatively simple geometry allowed for analytical solutions. The graphene wrinkling assumes a conformation, with the largest possible χ, that tends to reach an equilibrium state corresponding to a (local) minimum of the elastic energy as a basis for the physical solution. For simplicity, it is assumed

that the protrusions have comparable size and then the wrinkle sags in the middle. In the deformed region, or the x projection of the wrinkling region (i.e., $|x| \leqslant \chi/2$), the elastic energy is expressed as a summation of the stretching energy and the bending energy

$$\mathcal{E}(\zeta) = \frac{E_{2D}}{8}(\pi - \theta)\left[\frac{1}{\sin(\theta/2)} - 1\right]^{-1} \int \zeta(\partial_x \zeta)^4 dx$$
$$+ \frac{\kappa}{2}(\pi - \theta)\left[\frac{1}{\sin(\theta/2)} - 1\right] \int \zeta^{-1} dx. \quad (3)$$

The adhesion energy to the substrate is given by

$$E_{\text{adh}} = 2\Gamma \chi d \tan(\theta/2), \quad (4)$$

where Γ is the graphene-SiO$_2$ adhesion energy per area. At the contact between graphene and the substrate, graphene is bent with an equilibrium curvature $\mathcal{C}_{\text{eq}} = (2\Gamma/\kappa)^{1/2}$ [9]. The bending and the adhesion energies at the foot of the wrinkle are, respectively,

$$E_b = \chi\left(\frac{\Gamma\kappa}{2}\right)^{1/2}(\pi - \theta),$$
$$E_a = 2\Gamma\chi\mathcal{C}_{\text{eq}}^{-1}\tan\beta = \chi(2\Gamma\kappa)^{1/2}\tan\left(\frac{\pi - \theta}{4}\right). \quad (5)$$

Here 2β is the angle of the curved region (see Fig. 1).

By using the total energy $E = \mathcal{E} + E_{\text{adh}} + E_b + E_a$, one sees that the equilibrium elastic equation or the Euler-Lagrange equation for the wrinkling graphene can be written in the form

$$\zeta^2[3(\partial_x \zeta)^4 + 12\zeta(\partial_x \zeta)^2 \partial_{xx}\zeta] + \lambda^2 = 0, \quad (6)$$

in which

$$\lambda = \sqrt{\frac{4\kappa}{E_{2D}}}\left[\frac{1}{\sin(\theta/2)} - 1\right] = \frac{h}{\sqrt{3}}\left[\frac{1}{\sin(\theta/2)} - 1\right]. \quad (7)$$

Parameter λ, which tends to 0 in the limit of small graphene thickness, can be used to highlight the importance of the ratio of the bending rigidity to the tensile rigidity. In fact, parameter λ, which is proportional to h, can be used as a small parameter, instead of h, for an expansion scheme. This question will be addressed in the next section. The physical reason is that we expect singular behaviors of ζ in the small λ limit.

The equilibrium equation has to be solved with the boundary conditions

$$\zeta(\pm\chi/2) = 0, \quad (8)$$

where ridge length χ is unknown and must itself be determined in solving the problem. The mirror symmetry of the equilibrium equation and boundary conditions suggest that the equilibrium solution can also be symmetric, i.e., $\zeta(-x) = \zeta(x)$. This is the problem that was studied by Yammoto *et al.* and that we are going to deal with. In particular, our aim is to investigate the critical (or the maximal) nanoparticle separation χ_c above which the graphene sheet delaminates instead of wrinkling.

Note that Eq. (6) is degenerate in the sense that the coefficient $\zeta^3(\partial_x \zeta)^2$ of the highest-order derivative $\partial_{xx}\zeta$ vanishes at $\zeta = 0$ or $\partial_x \zeta = 0$. Therefore, the problem may have boundary layer solutions [10] or/and solutions which are

not necessary in the class of Lipschitzian functions, and that the equilibrium equation may have no mathematically convenient solution as is shown for some variational problems [11].

In order to gain some insight into the singularity of Eq. (6), we may look at local properties of solutions at $x = 0$ (a possible singular point). We then assume as a first approximation

$$\zeta = \zeta_0(1 + a|x|^\alpha) + o(|x|^\alpha) \quad (9)$$

for small x, in which $\zeta_0, \alpha > 0$, and a are real parameters. By substituting (9) into (6) we get $\alpha = 4/3$ and $a = -\zeta_0^{-2}(3/4)^{4/3}(\lambda^2/3)^{1/3}$. Hence, we may expect that the equilibrium equation has only piecewise C^2 solutions with continuation of the first derivative across each breaking point.

The main contribution of this paper is to rigorously obtain all pairs (ζ, χ) satisfying (6)–(8) and to select the critical pair (ζ_c, χ_c), or the real equilibrium solution, corresponding to the maximal length of the wrinkle (the optimum solution) and to a (local) minimizer of the total energy E.

First, we find that the wrinkling profile can be fully determined by solving the following equation [see Eq. (A3)]:

$$\zeta^2(\partial_x \zeta)^4 - \mathcal{D}\zeta = \frac{\lambda^2}{3}, \quad (10)$$

in which

$$\mathcal{D} = \zeta_0(\gamma)^4 - \frac{\lambda^2}{3}\zeta_0^{-1}, \quad (11)$$

where

$$\zeta(0) = \zeta_0, \quad \partial_x \zeta(0) = \gamma. \quad (12)$$

Parameters ζ_0 and γ can be viewed as shooting or input parameters. The above equation is called the Beltrami identity (1868) or Du Bois-Reymond equation (1879) for E. Despite its simplicity, the Beltrami equation need not have a physical solution for any $\mathcal{D}$.

Note that constant $\mathcal{D}$ reflects some competition between ζ_0 (the maximum deflection) and γ (the slope deflection at $x = 0$). Equation (10) will be investigated for different values of parameters ζ_0 and γ. In fact, our main concern is to know for which pairs $(\zeta_0, \gamma), 0 < \zeta_0 \leqslant d$, the associated solution satisfies the boundary conditions and has the largest distance between nanoparticles, which fully agrees with the physical intuition. Once problem (6)–(8) is solved, parameter θ can be selected through minimization of the total energy E.

One simple but important remark derived from (10) is that the elastic energy for the deformed membrane then becomes

$$\mathcal{E}(\zeta) = \frac{2\kappa}{3}(\pi - \theta)\left[\frac{1}{\sin(\theta/2)} - 1\right]\int \zeta^{-1} dx$$
$$+ \frac{E_{2D}}{8}(\pi - \theta)\left[\frac{1}{\sin(\theta/2)} - 1\right]^{-1}\chi\mathcal{D}. \quad (13)$$

Hence, it is tempting to conclude naively that the membrane has to adopt the largest possible deflection in order to minimize the elastic energy.

IV. WRINKLING MORPHOLOGY

The aim of this long section is to obtain all solutions in mathematical terms that may result from the simplified

equilibrium equation (10), keeping in mind that the purpose of the paper is to find stationary-energy deflections for different physical parameters in the context of graphene instability and to predict the critical distance between two nanoparticles.

A. Energetic argument

It is worth mentioning that the critical ridge length can be estimated by using the classical scaling argument. At the lowest order the stretching energy is of order $E_{str} \sim E_{2D}\epsilon^2 \chi W_{av}$, where ϵ is the stretching strain satisfying $\epsilon \sim \zeta_0^2/\chi^2$, $0 < \zeta_0 \leqslant d$, and W_{av} is the average width of the wrinkling profile. Bending energy E_{ben} is proportional to the curvature ($\sim \zeta_0/\chi^2$) squared, so $E_{ben} \sim \kappa(\zeta_0/\chi^2)^2 \chi W_{av}$. The adhesion energy is of order $E_{adh} \sim \Gamma \chi W_{av}$. Therefore, the total energy can be approximated by

$$E \sim E_{2D}\frac{\zeta_0^4}{\chi^3}W_{av} + \kappa\frac{\zeta_0^2}{\chi^3}W_{av} + \Gamma \chi W_{av}. \tag{14}$$

In passing, it may be noted that from the ratio $E_{ben}/E_{str} \sim \kappa/\zeta_0^2 E_{2D}$ we can deduce a size scale

$$d^\star = \sqrt{\frac{\kappa}{E_{2D}}} = \frac{\sqrt{3}}{6}h, \tag{15}$$

which determines a bending-dominated regime ($E_{str} \ll E_{ben}$) if $d \ll d^\star$ and a stretching-dominated regime ($E_{str} \gg E_{ben}$) if $d \gg d^\star$.

In view of (14), a critical wrinkle length is simply obtained by minimizing the right-hand side of (14) with respect to χ. We find $\chi^c = (3[E_{2D}\zeta_0^4 + \kappa\zeta_0^2]/\Gamma)^{1/4}$, irrespective of the average width of the wrinkling profile. Therefore, the maximum wrinkle length satisfies

$$\chi_c = \left(3\frac{E_{2D}d^4 + \kappa d^2}{\Gamma}\right)^{1/4}. \tag{16}$$

Equation (16) can be used to determine a phase diagram showing a possibility of a transition between wrinkling and partial or complete delamination in the parameter space of ridge length and nanoparticle size.

Note that for $d \ll d^\star$, we have

$$\chi_c \sim (3\kappa/\Gamma)^{1/4}d^{1/2} \equiv \chi_c^b, \tag{17}$$

and in the opposite situation ($d \gg d^\star$), χ_c satisfies, as in Ref. [4],

$$\chi_c \sim (3E_{2D}/\Gamma)^{1/4}d \equiv \chi_c^s. \tag{18}$$

The above critical lengths are analogous to the critical blister radii of a thin elastic sheet adhering to a stiff substrate by means of the surface tension of a thin liquid layer [12].

Next, since χ_c^b and χ_c^s coincide if (and only if) $d = d^\star$, we can simply write the critical lines as

$$\chi_c = \begin{cases} (3\kappa/\Gamma)^{1/4}d^{1/2}, & \text{if } d < d^\star, \\ (3E_{2D}/\Gamma)^{1/4}d, & \text{if } d > d^\star, \end{cases} \tag{19}$$

instead of (16). This can be used as a first-order approximation of the critical line for the possibility of a wrinkling-delamination transition in the parameter space of ridge length and nanoparticle size [in the intermediate region
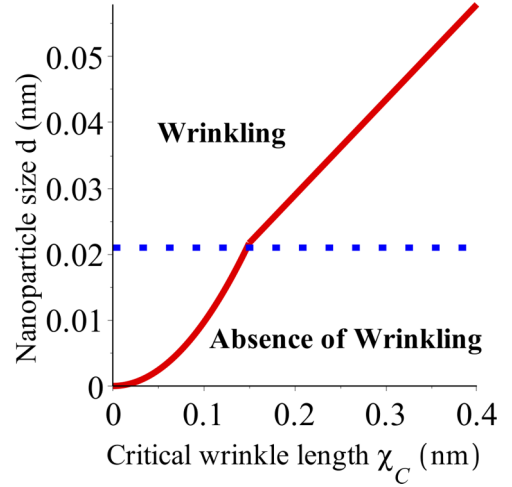
FIG. 2. Nanoparticle size as a function of critical wrinkling length for both bending-dominated regime and stretching-dominated regime (solid red line). Physical parameters are $E_{2D} = 2.12 \times 10^3$ eV/nm^2, $\Gamma = 2.8$ eV/nm^2, and $\kappa = 1$ eV. The horizontal dotted blue line shows $d = d^\star = 0.021$ nm, which separates the two dominated regimes.

between bending-dominated regime and stretching-dominated regime we can use (16)]. In Fig. 2 we have plotted the nanoparticle size as a function of χ_c by using (19). Similar results were obtained for the pinning of a two-dimensional membrane to a patterned substrate (see Fig. 2 of Ref. [13]). Figure 2 can also be interpreted as a diagram of the wrinkling instability of graphene on a substrate-supported silica nanoparticle.

Equation (19) also shows that the dependence of the nanoparticle size is quadratic if $\chi_c < (3\kappa^2/\Gamma E_{2D})^{1/4} = \chi_c^\star$ (bending-dominated regime), and this dependence is linear if $\chi_c > \chi_c^\star$ (stretching-dominated regime). For the values $E_{2D} = 2.12 \times 10^3$ eV/nm^2, $\Gamma = 2.8$ eV/nm^2, and $\kappa = 1$ eV, given in Ref. [4], the calculation predicts that $\chi_c^\star = 0.149$ nm, which is of the order of the lattice spacing $a = 0.142$ nm (for flat graphene). This prediction would imply, as mentioned in Ref. [13], that the bending-dominated regime is greatly suppressed.

Let us note that the case $d \ll d^\star$ occurs in multilayer graphene for which we find structural transitions from conformal adhesion to wrinkling to delimitation with increasing graphene thickness (or nanoparticle density ρ_{np}). Interestingly, in the bending-dominated model it is shown that unbinding is controlled by a single dimensionless parameter $\alpha = (2\Gamma_n/\kappa_n)^{1/4}/(4\pi^2\rho_{np}d)^{1/2}$ [4,14], where κ_n is the bending rigidity of n-layer graphenes for $n > 1$ and Γ_n is the adhesion energy between SiO$_2$ and n-layer graphene. Γ_n is assumed to be independent of n. For small enough α, partial or total unbinding is predicted, while for large α the graphene membrane is expected to conform to the substrate (except for small regions around the nanoparticles) [14]. For fixed $n > 1$, unbinding threshold occurs at some $\alpha = \overline{\alpha}$ [4], which intuitively has to satisfy $\overline{\alpha} = (2\Gamma_n/\kappa_n)^{1/4}/(4\pi^2\rho_c d)^{1/2}$, where ρ_c is the threshold density. Using (17) one sees that $\rho_c\chi_c^2 \sim 1/2\pi^2\overline{\alpha}^2$, which is in a reasonable agreement with [4] (i.e., ρ_c is of order χ_c^{-2}).

B. Solving the Beltrami equation

According to the continuum model if $\gamma = 0 \, [= \partial_x \zeta(0)]$, i.e., $3\mathcal{D}/\lambda^2 = -\zeta_0^{-1}$, there exists a real number $0 < \chi(\zeta_0) \leqslant \infty$ (not necessarily finite) such that the Beltrami equation has a unique nontrivial smooth solution ζ [see Eqs. (A4) and (A5)] such that $\zeta(\pm\chi(\zeta_0)/2) = 0$; that is, for a catenary-like profile the critical deflection is smooth, satisfies, for $x > 0$,

$$x = \zeta_0^{3/2}\left(\frac{\lambda^2}{3}\right)^{-1/4}\int_{\zeta(x)/\zeta_0}^1 \frac{\sqrt{s}\,ds}{(1-s)^{1/4}} \qquad (20)$$

and, then, $\chi(\zeta_0)$ has the expression

$$\chi(\zeta_0) = 2\zeta_0^{3/2}\left(\frac{\lambda^2}{3}\right)^{-1/4}\int_0^1 \frac{\sqrt{s}\,ds}{(1-s)^{1/4}}, \qquad (21)$$

which is finite and monotonically increases with ζ_0 as $\zeta_0^{3/2}$. The integral in Eq. (21) is the known Eulerian integral of the first kind or the complete beta function $\beta(3/2, 3/4)$ [see Eq. (A8)].

It should be noticed that $\chi(\zeta_0)$ can also be written as

$$\chi(\zeta_0) = 2\zeta_0^{3/2}\left(\frac{\lambda^2}{3}\right)^{-1/4}\int_1^\infty \frac{ds}{s^{3/2}(s-1)^{1/4}}, \qquad (22)$$

and for given ζ_0 and γ (such that $\mathcal{D} < 0$), the associated distance between two nanoparticles satisfies

$$\chi(\zeta_0, \gamma) = 2\zeta_0^{3/2}\left(\frac{\lambda^2}{3}\right)^{-1/4}\int_1^\infty \frac{ds}{s^{3/2}\big(s - 1 + 3\zeta_0^2\gamma^4/\lambda^2\big)^{1/4}}, \qquad (23)$$

from which it is clearly seen that the function $\gamma \to \chi(\zeta_0, \gamma)$ is maximal at $\gamma = 0$, i.e., $\chi(\zeta_0) = \chi(\zeta_0, 0)$. Our analysis showed that for a given χ there exists a unique $\mathcal{C}^1$ smooth deflection for which the maximum deflection $\zeta_0 = \zeta(0)$, as a function of the distance between nanoparticles, is given by

$$\zeta_0 = \chi^{2/3}(\lambda^2/3)^{1/6}/\overline{\chi}^{2/3}, \quad \overline{\chi} = 2\beta(3/2, 3/4) \approx 1.917. \qquad (24)$$

The maximum deflection ζ_0 monotonically increases with χ as $\chi^{2/3}$. Equation (24) follows the same (general) trend as in Eq. (2). Next, since the goal is to make the distance between nanoparticles as large possible, one deduces that the maximum wrinkle length is given by

$$\chi(d) = d^{3/2}(3/\lambda^2)^{1/4}\overline{\chi} \approx 1.917 d^{3/2}(3/\lambda^2)^{1/4}. \qquad (25)$$

For ease of comparison with the results obtained in Ref. [4], we note that in the limit $\mathcal{D} = 0$, we recover the results of Ref. [4]. Indeed, in this limit, Eq. (10) reads

$$\zeta^2(\partial_x\zeta)^4 = \frac{\lambda^2}{3}, \qquad (26)$$

from which one can deduce nanoparticle separation χ^{ex} derived in Ref. [4] [see Eq. (2)] and that the corresponding solution can be written in the explicit form

$$\zeta^{\mathrm{ex}}(x) = \left(\frac{3}{2}\right)^{2/3}\left(\frac{\lambda^2}{3}\right)^{1/6}\left[\frac{2}{3}\left(\frac{3}{\lambda^2}\right)^{1/4}\zeta_0^{3/2} - |x|\right]^{2/3}, \qquad (27)$$

as described by Eqs. (1) and (2).

With the previous calculation, we note that χ^{ex} can be rewritten as

$$\chi^{\mathrm{ex}}(\zeta_0) = \frac{4}{3\overline{\chi}}\chi(\zeta_0) \approx 0.695\chi(\zeta_0), \qquad (28)$$

which is clearly lower than $\chi(\zeta_0)$.

In Ref. [4], it is estimated that the maximal length (with $\zeta_0 = d = 7.4 \pm 2.2$ nm) is $\chi^{\mathrm{ex}} = 104 - 65$ nm along with $\theta = 35° - 14°$ for $\Gamma = 0.6\text{–}2.8$ eV/nm^2, respectively, in rough agreement with the observed maximum wrinkle length of approximately 200 nm. Using (28) instead provides a relatively better result. Since $\chi(\zeta_0) \approx 1.438\chi^{\mathrm{ex}}(\zeta_0)$, the maximal length is estimated to be $\chi \approx 149.5\text{–}93.4$ nm. However, our analytical prediction also underestimates the maximum wrinkle length. This is not unexpected due to the fact that our work is based on the physical model of Ref. [4], which does not incorporate the possibility of finite size effects. For simplicity, it is also assumed that the protrusions have comparable heights (therefore, the wrinkle sags in the middle), and that the opening angle is uniform. In addition, because of the random distribution of the nanoparticles, it is possible that the interaction between ridges could influence the critical nanoparticle separation (boundary-layer solution) and introduce some complicated boundary conditions. Last, other physical mechanisms (such as impurities at the substrate surface, defects, thermal fluctuations, and more) can also be considered as possible sources of the discrepancy between the analytical predictions and experiments. An attempt to understand graphene responses with regard to those various contexts goes beyond the scope of the present paper. Nevertheless, some insight can be gained with the help of the existing theory of Ref. [4] via a rigorous analysis. The merit of the present simple elastic model, which includes a minimal set of physical ingredients, allows for an analytic solution. More realistic models can then be proposed step by step if one wishes to have a more quantitative comparison with experiments. The present level of analysis provides a theoretical framework in which we show the possibility of a graphene wrinkling where the geometry parameters of the nanoparticle, i.e., the size and separation, act as control parameters. Globally, our results, which agree with the energetic argument presented above, improve the elastic analysis of Ref. [4] and seem to be sufficient, at least in the first approximation, for testing the degree to which the nanoparticle size influences the wrinkle length.

To summarize, the graphene is deflected in a smooth manner, and the maximum wrinkle length χ_c is explicitly given by [see (25)]

$$\chi_c = d^{3/2}\left(\frac{3E_{2\mathrm{D}}}{4\kappa}\right)^{1/4}\left[\frac{1}{\sin(\theta/2)} - 1\right]^{-1/2}\overline{\chi}, \qquad (29)$$

depending only on the model. What is surprising is that our analysis, which has a remarkable degree of simplicity, showed that χ_c can be determined explicitly without assuming prior knowledge of the deflection profile. By minimizing the total energy as a function of θ, we will derive the linearity of the relation between d and the critical maximum wrinkle length. A detailed of the scaling law for the critical separation is provided in Appendix B.

C. Asymptotic deflection in the limit $\lambda \to 0$

In the previous sections, we studied the wrinkling of graphene for which the effects of the bending and the stretching are present. However, from Fig. 2, we can notice that the critical nanoparticle size for which the bending rigidity is relevant is small ($d^\star = 0.021$ nm). Therefore, since the diameter of the silica nanoparticles is shown to be $d = 7.4 \pm 2.2$ nm, which is large relative to $d^\star$, we may deduce that wrinkling due to the stretching cost is to be expected. The goal of this section is to derive an approximate solution to the equilibrium equation for small values of λ. This case occurs when the stretching which accompanies the bending of the graphene is a first-order effect in comparison with the bending ($d \gg d^\star$). We assume that the continuum model can be applied in this limit. The solution will be sought as an expansion in power of λ^2:

$$\zeta = \zeta^0 + \lambda^2 \zeta^1 + \cdots. \tag{30}$$

According to (11), it makes sense to assume

$$\mathcal{D} = \mathcal{D}_0 + \lambda^2 \mathcal{D}_1 + \cdots. \tag{31}$$

Inserting the above series into the Beltrami equation we get, at leading order,

$$\zeta^0 (\partial_x \zeta^0)^4 = \mathcal{D}_0, \tag{32}$$

and, at the first order,

$$4(\zeta^0)^2 (\partial_x \zeta^0)^3 \partial_x \zeta^1 + \mathcal{D}_0 \zeta^1 - \mathcal{D}_1 \zeta^0 - \tfrac{1}{3} = 0, \tag{33}$$

which is a linear ordinary differential equation for ζ^1. This equation still contains undetermined parameters $\mathcal{D}_0$ and $\mathcal{D}_1$ and also contains the unknown function ζ^0, which must be first determined from leading order equation (32).

To solve (32), we note that $\mathcal{D}_0$ has to be $\mathcal{D}_0 = \zeta_0(\gamma)^4$, where $\zeta_0 = \zeta^0(0)$ and $\gamma = \partial_x \zeta_0(0)$. Together with Eq. (32), we deduce that the (critical) approximate solution is given by

$$\zeta^0(x) = \left(\frac{5}{4}\right)^{4/5} d^{1/5} |\gamma|^{4/5} \left(\frac{\chi^0}{2} - |x|\right)^{4/5}, \tag{34}$$

where

$$\chi^0 = 8|\gamma|^{-1} d / 5. \tag{35}$$

To solve (33), we use the expression for ζ^0 to deduce an exact expression for the general solution,

$$\zeta^1 = \frac{1}{3} d^{-1} |\gamma|^{-4} + \mathcal{D}_1 \left(\frac{4}{5}\right)^{1/5} |\gamma|^{-16/5} \left(\frac{\chi^0}{2} - |x|\right)^{4/5}$$
$$+ c \left(\frac{\chi^0}{2} - |x|\right)^{-1/5}, \tag{36}$$

where c is an arbitrary constant. Note that ζ^1 diverges at $x = \pm \chi^0/2$, except if $c = 0$.

Here we notice, as pointed out in Ref. [10], that there is no reason to expect that the approximate solution satisfies the boundary conditions or/and that χ^0 coincides with the critical distance χ_c obtained in Sec. 4.1. In fact, a leading order solution might be a good approximation only in a restricted region away from the boundary.

D. Pseudomagnetic fields

We briefly here investigate electronic property responses to the wrinkling of graphene. It has been found that a strain can induce gauge fields that effectively act as a magnetic field on the electronic structure of graphenes depending on the patterned substrate [5,16,17]. In Ref. [17], the authors observed that these effective pseudomagnetic fields can exceed 300 T for graphene nanobubbles on Pt(111) single-crystal substrates.

According to Refs. [5] and [13], Yamamoto *et al.* argued that the pseudomagnetic field can be simply given by

$$B_{\text{eff}} \approx \frac{\Phi_0 \beta}{a W} (\partial_x \zeta)^2, \tag{37}$$

where $\Phi_0 = 10^{-15}$ Wb is the flux quantum, $\beta \approx 2$ the change in the hopping amplitude between the neighboring atomic sites due to the lattice deformation, a ($=0.142$ nm) the lattice constant, and W the typical wrinkle width. Quantity $(\partial_x \zeta)^2 = \epsilon_x$ represents the strain distribution along a wrinkle described by deflection profile ζ. By using the explicit solution (1), it has been found that the minimum pseudomagnetic field is of order 10 T for $\chi = 100$ nm [4].

Here we use expression (37) to evaluate the pseudomagnetic field at the middle of the wrinkled graphene by using our analytical results. First, we consider the case of small λ and use the approximate solution (34). At $x = 0$, since $\partial_x \zeta^0(0) = \gamma_c^0$ [see Eq. (B13)], we obtain

$$B_{\text{eff}} \approx 4 \frac{\Phi_0 \beta}{a W} \left(\frac{\Gamma}{3 E_{\text{2D}}}\right)^{1/2} (\pi - \theta)^{-1/2}$$
$$\times \left[\frac{1}{\sin(\theta/2)} - 1\right]^{1/2} \tan^{1/2}(\theta/2). \tag{38}$$

For θ small enough, we have

$$B_{\text{eff}} \approx 4 \frac{\Phi_0 \beta}{a W} \left(\frac{\Gamma}{3 \pi E_{\text{2D}}}\right)^{1/2}, \tag{39}$$

from which we obtain a B_{eff} of order 302 T for the wrinkle width $W = 1.1$ nm and for $E_{\text{2D}} = 2.12 \times 10^3$ eV/nm^2, $\Gamma = 2.8$ eV/nm^2. Interestingly, in the case where the elastic behavior of graphene on a nanoparticle is predominantly determined by stretching, Yamamoto *et al.* [4] have estimated that the maximum pseudomagnetic field B_{eff} is of order 300 T at the radial distance $d/2$ (from the middle) for $d = 7.4$ nm, in the absence of wrinkling, corresponding to small thickness or small nanoparticle density.

For the case where the bending rigidity is not neglected compared to tensile rigidity, one sees from (A4) that the distribution of the pseudomagnetic field acting on the electrons can be expressed in terms of the wrinkling deflection:

$$B_{\text{eff}}(x) \approx \frac{\Phi_0 \beta}{a W} \left(\frac{\lambda^2}{3}\right)^{1/2} d^{-1/2} \zeta^{-1} [d - \zeta]^{1/2}. \tag{40}$$

The above equation shows that the pseudomagnetic field is not uniform and depends on the spacial distribution of the deflection. Note that the pseudomagnetic field diverges near particles as $B_{\text{eff}}(x) \approx (\chi_c/2 \pm x)^{-2/3}$. In fact, as noted in Ref. [4], the pseudomagnetic field near particles in the wrinkled graphene will generally be more complicated depending on the particle and their direction with respect to each other and the lattice. At

the middle $x = 0$ since $\zeta(0) = d$, we find by using expression (40), that the wrinkling graphene described by the present critical deflection may have a zero pseudomagnetic field irrespective of the nanoparticle size and wrinkle width, at odds with Ref. [4], even if our finding should not be generalized for any deflected wrinkles, as shown in Eq. (39).

V. CONCLUSION

The present work has the main objective to theoretically analyze a simple continuum model describing the wrinkling of graphene on a substrate decorated with silica nanoparticles having comparable heights. We have showed that a wrinkle formed between two protrusions can be described in terms of a $\mathcal{C}^1$ smooth deflection. We have also determined *a priori,* as a function of the nanoparticle size, an explicit expression of the maximum wrinkle length below which a wrinkling is induced (i.e., for a given nanoparticle size the graphene membrane wrinkles if the distance between two nanoparticles is not larger than χ_c). Finally, from the present continuum elastic theory, we have derived an expression of the pseudomagnetic filed as a function of the wrinkling deflection and concluded that the middle of the wrinkling graphene may have a zero pseudomagnetic field. Naturally, they still open interesting questions concerning the limitations of the continuum model. However, we believe that the present results can be used as a starting basic solution for a more general picture of the wrinkling of graphene on nanoparticles, including the case where nanoparticles have different heights and/or the random distribution of the nanoparticles by adding noise to the model.

APPENDIX A: THE BELTRAMI EQUATION

We discuss the technical details of the analysis of the equilibrium equation and derive an expression of deflection ζ. First, we use the coordinate system $\psi = \zeta^{3/2}$ and $v = \partial_x \psi$. Accordingly, Eq. (6) is transformed into the system

$$\partial_x \psi = v,$$
$$\partial_x v = 9(2^4 3^{-3} v^4 - \lambda^2)/2^5 \psi v^2. \qquad (A1)$$

It is easy to see that system (A1) has the following first integral:

$$\frac{\psi}{|3(2/3)^4 v^4 - \lambda^2|^{3/2}} = c, \qquad (A2)$$

where c is a constant, which can be written as

$$(\partial_x \zeta)^4 = \zeta^{-1} \left(\frac{\lambda^2}{3} \zeta^{-1} + \mathcal{D} \right), \qquad (A3)$$

from which one obtains the Beltrami equation (10)–(12).

Now, we are going to solve the simplified equilibrium equation by using a phase-plane analysis. This approach will provide explicit results of the deflection profile and a way to derive easily an exact expression of χ_c. In Fig. 3 we illustrate the dependence on parameter $\mathcal{D}$ appearing in Eq. (10). Two families of (mathematical) solutions are observed. When $\mathcal{D} \geqslant 0$, for any (ζ_0, γ) in the first quadrant $\zeta_0 > 0, \gamma > 0$, (resp. the second quadrant $\zeta_0 > 0, \gamma < 0$), the orbit $(\zeta, \partial_x \zeta)$ remains in this quadrant (resp. in the second quadrant).

If $\mathcal{D} < 0$, any curve $(\zeta, \partial_x \zeta)$ initially in the first quadrant enters the second quadrant through the half line
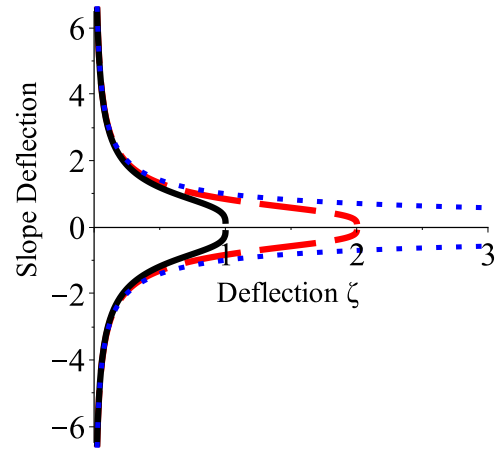
FIG. 3. Plots of $\partial_x \zeta$ vs ζ according to (10) in arbitrary units. Different curves refer to different choices of the quantity $\mathcal{D} = \zeta_0 \gamma^4 - \lambda^2/(3\zeta_0)$ and show that a condition for a bounded solution is $\mathcal{D} < 0$. Here parameters are $\lambda = \sqrt{3}$, $\mathcal{D} = 0$ for the dotted blue line, -1 for the solid black line, and -0.5 for the dashed red line.

$\{(\zeta, q) : \zeta > 0, q = 0\}$, in the direction of decreasing ζ, and remains there. Therefore, $\partial_x \zeta$ changes sign and has exactly one zero. Under the assumption that $\zeta_0 = \zeta(0)$ is the maximum deflection, we have necessarily $\gamma = 0$ and there exists a real number $0 < \chi(\zeta_0) \leqslant \infty$ such that ζ is increasing on $(-\chi(\zeta_0)/2, 0)$, decreasing on $(0, \chi(\zeta_0)/2)$, and vanishing at $x = \pm\chi(\zeta_0)/2$.

Next, by using Eq. (A3), with $3\mathcal{D}/\lambda^2 = -\zeta_0^{-1}$, the Beltrami equation reads

$$\partial_x \zeta = \pm \left(\frac{\lambda^2}{3} \right)^{1/4} \zeta^{-1/4} [\zeta^{-1} - \zeta_0^{-1}]^{1/4}, \qquad (A4)$$

from which one sees, for $x > 0$,

$$x = \zeta_0^{3/2} \left(\frac{\lambda^2}{3} \right)^{-1/4} \int_{\zeta(x)/\zeta_0}^{1} \frac{\sqrt{s}\, ds}{(1-s)^{1/4}}. \qquad (A5)$$

This shows in particular that the Beltrami equation with $3\mathcal{D}/\lambda^2 = -\zeta_0^{-1}$ has a unique nontrivial smooth solution (cf. Amann [15, p. 67]).

Note that deflection ζ can also be written as a solution to the following inversion problem:

$$I_{\zeta(x)/\zeta_0}(3/2, 3/4) = 1 - \frac{2|x|}{\chi(\zeta_0)}, \qquad (A6)$$

where $\chi(\zeta_0)$ is given by (22) in the main text, $I_z(3/2, 3/4)$ [Person's (1934) notation] is the normalized (or regularized) incomplete beta function

$$I_z(a, b) = \frac{1}{\beta(a, b)} \int_0^z s^{a-1} (1-s)^{b-1} ds = \frac{\beta_z(a, b)}{\beta(a, b)}, \qquad (A7)$$

for $0 < z < 1$, and for arbitrary argument $a > 0, b > 0$, where

$$\beta(a, b) = \beta_1(a, b) = \int_0^1 s^{a-1} (1-s)^{b-1} ds. \qquad (A8)$$

The normalized incomplete beta function is one of the most important distributions in probability and statistics and is a standard special function of mathematical physics. $I_z(a, b)$ is

also called the cumulative distribution function and is related to the cumulative binomial distribution (see, e.g., Ref. [18]). The (non-normalized) beta function $\beta(a,b)$ has played an important instrumental role in the original formulation of string?brk?> theory [19].

Next, by using the property $I_z(a,b) = 1 - I_{1-z}(a,b)$, one can see that ζ has the following explicit form expressed in terms of the inverse of the normalized incomplete beta function:

$$\zeta = \zeta_0\big[1 - I_{2|x|/\chi(\zeta_0)}^{-1}(3/4,3/2)\big]. \qquad (A9)$$

Although the normalized incomplete beta function and its inverse do not fall into the category of elementary functions, they are standard special functions of mathematical physics.

$$E_{\text{tot}} = \left(\frac{3d^2 E_{2D}}{4\kappa}\right)^{1/4}\left\{\frac{r\kappa}{3^{5/4}}(\pi - \theta)\left[\frac{1}{\sin(\theta/2)} - 1\right]^{1/2} + 2\Gamma\overline{\chi}d^2\left[\frac{1}{\sin(\theta/2)} - 1\right]^{-1/2}\tan(\theta/2)\right.$$

$$\left. + d\overline{\chi}\sqrt{\Gamma\kappa}\left[\frac{1}{\sin(\theta/2)} - 1\right]^{-1/2}\left[2^{-1/2}(\pi - \theta) + 2^{1/2}\tan\left(\frac{\pi - \theta}{4}\right)\right]\right\}, \qquad (B1)$$

where r is an universal number satisfying $r \geqslant 3^{5/4}/(2\overline{\chi})$, and where we have used the critical deflection with the exact expression (29) for the critical separation. However, the expression of E_{tot} makes the minimization problem impossible to solve analytically. Therefore, for any analytical progress the critical opened angle which minimizes E_{tot} will be evaluated in two opposite regimes that are of particular interest, depending on whether $\mathcal{C}_{\text{eq}}d \gg 1$ or $\mathcal{C}_{\text{eq}}d \ll 1$. For intermediate regimes the opened angle has to be chosen only numerically.

On the other hand, we anticipate that at the critical opened angle all terms of E_{tot} are comparable. In particular, quantity $(\pi - \theta)[1/\sin(\theta/2) - 1][\tan(\theta/2)]^{-1}$ has to be proportional to $2\Gamma d^2/\kappa$:

$$(\pi - \theta)[1/\sin(\theta/2) - 1][\tan(\theta/2)]^{-1} = \text{constant} \times \big(\mathcal{C}_{\text{eq}}d\big)^2. \qquad (B2)$$

For the strong adhesion limit ($\mathcal{C}_{\text{eq}}d \gg 1$), we deduce that θ goes to zero. Hence, in place of $\sin(\theta/2)$ we take $\theta/2$, so that the total energy can be approximated by

$$E_{\text{tot}} \sim \left(\frac{3d^2 E_{2D}}{4\kappa}\right)^{1/4}[\nu_1\theta^{-1/2} + \nu_2\theta^{3/2} + \nu_3\theta^{1/2}], \quad (B3)$$

where

$$\nu_1 = 2^{1/2}\frac{r\kappa}{3^{5/4}}\pi, \quad \nu_2 = 2^{-1/2}\Gamma\overline{\chi}d^2,$$

$$\nu_3 = d\overline{\chi}(\Gamma\kappa)^{1/2}\frac{\pi + \sqrt{2}}{2}.$$

Therefore, the critical opened angle is given by

$$\theta_c = \sqrt{\frac{\nu_1}{3\nu_2}}\left[\sqrt{1 + \frac{\nu_3^2}{12\nu_1\nu_2}} - \frac{\nu_3}{\sqrt{12\nu_1\nu_2}}\right]$$

$$= \frac{2}{3^{9/8}}\sqrt{\frac{r\pi}{\overline{\chi}}}(\mathcal{C}_{\text{eq}}d)^{-1}\mathcal{Z}, \qquad (B4)$$

$I_z(a,b)$ and $I_z^{-1}(a,b)$ have been extensively investigated from different point of view and are readily computable.

Therefore, the critical (smooth) deflection can be uniquely given by ($\zeta_0 = d$)

$$\zeta^c = d\big[1 - I_{2|x|/\chi(d)}^{-1}(3/4,3/2)\big]. \qquad (A10)$$

APPENDIX B: SCALING ANALYSIS FOR χ_c

In this section, we derive the scaling law for the critical nanoparticle separation as in Ref. [4]. Up to now, we have implicitly assumed that θ can vary arbitrary. In fact, the selected graphene shape must have an opened angle minimizing the total energy, which reads, as a function of θ,

where $\mathcal{Z}$ is an universal parameter given by $\mathcal{Z} = \left[\sqrt{1 + (\pi + 2^{1/2})^2\frac{3^{1/4}\overline{\chi}}{16r\pi}} - (\pi + 2^{1/2})\frac{3^{1/2}}{4}\sqrt{\frac{\overline{\chi}}{r\pi}}\right]$. Note that (B4) is consistent with the assumption that $\mathcal{C}_{\text{eq}}d \gg 1$. By using (B4) we deduce from (29)

$$\chi_c \sim d\left(\frac{E_{2D}}{\Gamma}\right)^{1/4}\left(\frac{r\pi 3^{3/4}\overline{\chi}^3}{72}\right)^{1/4}\sqrt{\mathcal{Z}}, \qquad (B5)$$

showing the linear dependence of χ_c on d, which is precisely what we had concluded from the energetic argument.

Note that in the case where the bending and adhesion energies at the foot of the wrinkle are neglected we have $\mathcal{Z} = 1$ and get simply

$$\theta_c = \frac{2}{3^{9/8}}\sqrt{\frac{r\pi}{\overline{\chi}}}(\mathcal{C}_{\text{eq}}d)^{-1},$$

$$\chi_c \sim d\left(\frac{E_{2D}}{\Gamma}\right)^{1/4}\left(\frac{r\pi 3^{3/4}\overline{\chi}^3}{72}\right)^{1/4}. \qquad (B6)$$

In the weak adhesion limit ($\mathcal{C}_{\text{eq}}d \ll 1$), the opened angle goes to π. Therefore,

$$E_{\text{tot}} \sim 2d^{1/2}\left(\frac{E_{2D}}{\kappa}\right)^{1/4}\left[\frac{r\kappa}{3}2^{-5/2}\Theta^2 + \Gamma 3^{1/4}\overline{\chi}d^2 2^{5/2}\Theta^{-2}\right.$$

$$\left. + 3^{5/4}\frac{d}{2}\overline{\chi}\sqrt{\Gamma\kappa}\right], \qquad (B7)$$

where $\Theta = \pi - \theta$. Arguing as above, one sees that the critical opened angle of the wrinkle satisfies

$$\theta_c \sim \pi - 2\left(\frac{3^{5/4}\overline{\chi}}{r}\right)^{1/4}(\mathcal{C}_{\text{eq}}d)^{1/2}, \qquad (B8)$$

and then

$$\chi_c \sim d\left(\frac{E_{2D}}{\Gamma}\right)^{1/4}(2r3^{3/4}\overline{\chi}^3)^{1/4}. \qquad (B9)$$

Our predicted results are similar to the scale laws reported in Ref. [4] with different (physical) prefactors, since their analysis used the explicit solution ζ^{ex} and the critical opened angle is calculated by assuming implicitly that the distance between two nanoparticles is independent of parameter θ, which is clearly not true. This also could explain the discrepancy, noticed in Ref. [4], between the theoretical predictions and the experiments.

Finally, we consider the case of small λ. First, we assume that the total energy can be expressed as a power of λ:

$$E_{\text{tot}} = E_{\text{tot}}^0 + \lambda E^1 + \cdots . \tag{B10}$$

To lowest order we obtain formally

$$E_{\text{tot}}^0 = \frac{E_{2D}}{8}(\pi - \theta)\left[\frac{1}{\sin(\theta/2)} - 1\right]^{-1} \int \zeta(\partial_x \zeta)^4 \, dx + 2\Gamma \chi d \tan(\theta/2), \tag{B11}$$

for which the associated Beltrami equation coincides with (32). By using the expression of the approximate solution ζ^0, the energy E_{tot}^0 is rewritten as

$$E_{\text{tot}}^0 = \frac{E_{2D}}{5}(\pi - \theta)\left[\frac{1}{\sin(\theta/2)} - 1\right]^{-1} d^2|\gamma|^3 + 16\Gamma d^2|\gamma|^{-1}\tan(\theta/2)/5. \tag{B12}$$

Therefore, ζ^0 has minimal energy if $\gamma = \gamma_c^0$, where

$$\left(\gamma_c^0\right)^4 = \frac{16}{3}\frac{\Gamma}{E_{2D}}(\pi - \theta)^{-1}\left[\frac{1}{\sin(\theta/2)} - 1\right]\tan(\theta/2), \tag{B13}$$

and then

$$\chi_c^0 = \frac{4}{5}3^{1/4}(\pi - \theta)^{1/4}\left[\frac{1}{\sin(\theta/2)} - 1\right]^{-1/4}$$
$$\times [\tan(\theta/2)]^{-1/4}\left(\frac{E_{2D}}{\Gamma}\right)^{1/4} d. \tag{B14}$$

This demonstrates the linear dependence (at leading order) of the critical length of the graphene on nanoparticle size.

As above, we consider two limiting cases. At small θ one has

$$\chi_c^0 \sim \frac{4}{5}3^{1/4}\pi^{1/4}\left(\frac{E_{2D}}{\Gamma}\right)^{1/4} d, \tag{B15}$$

which is similar to the scaling form of the maximum wrinkle length. Note that the above result is also similar to the result obtained in Ref. [4] for a stretching-dominated model by using Schwerin's solution for a membrane pushed by a point force [20]. Analogous scaling for the diameter detachment zones ($2R = \chi_c^0$) surrounding a local protuberance is discussed in Ref. [13]. For $\Theta = \pi - \theta$ small, we obtain again (B15).

[1] D.-Y. Khang, H. Jiang, Y. Huang, and J. A. Rogers, Science **311**, 208 (2006).

[2] Y. Sun, W. M. Choi, H. Jiang, Y. Y. Huang, and J. A. Rogers, Nat. Nanotechnol. **1**, 201 (2006).

[3] Y. Guo and W. Guo, J. Phys. Chem. C **117**, 692 (2013).

[4] M. Yamamoto, O. Pierre-Louis, J. Huang, M. S. Fuhrer, T. L. Einstein, and W. G. Cullen, Phys. Rev. X **2**, 041018 (2012).

[5] A. H. Castro Neto, F. Guinea, N. M. R. Peres, K. S. Novoselov, and A. K. Geim, Rev. Mod. Phys. **81**, 109 (2009).

[6] S. Zhu, J. Galginaitis, and T. Li, J. Nanomater. **2012**, 375289 (2012).

[7] S. Zhu and T. Li, J. Appl. Mech. **81**, 061008 (2014).

[8] A. Lobkovsky, S. Gentges, H. Li, D. Morse, and T. A. Witten, Science **270**, 1482 (1995).

[9] U. Seifert and R. Lipowsky, Phys. Rev. A **42**, 4768 (1990).

[10] A. E. Lobkovsky, Phys. Rev. E **53**, 3750 (1996).

[11] J. M. Ball and V. J. Mizel, Arch. Ration. Mech. Anal. **90**, 325 (1985).

[12] J. Chopin, D. Vella, and A. Boudaoud, Proc. R. Soc. London A **464**, 2887 (2008).

[13] S. Viola Kusminskiy, D. K. Campbell, A. H. Castro Neto, and F. Guinea, Phys. Rev. B **83**, 165405 (2011).

[14] O. Pierre-Louis, Phys. Rev. E **78**, 021603 (2008).

[15] H. Amann, Ordinary Differential Equations (Walter de Gruyter, Berlin, 1990).

[16] V. M. Pereira, A. H. Castro Neto, H. Y. Liang, and L. Mahadevan, Phys. Rev. Lett. **105**, 156603 (2010).

[17] N. Levy, S. A. Burke, K. L. Meaker, M. Panlasigui, A. Zettl, F. Guinea, A. H. Castro Neto, and M. F. Crommie, Science **329**, 544 (2010).

[18] D. Osborn and R. Madey, Math. Comp. **22**, 159 (1968).

[19] M. B. Green, J. H. Schwarz, and E. Written, Superstring Theory (Cambridge University Press, New York, 1987).

[20] E. Schwerin, Z. Angew. Math. Mech. **9**, 482 (1929).